

Stability of lipid bridges

This article has been downloaded from IOPscience. Please scroll down to see the full text article.

2001 J. Phys. A: Math. Gen. 34 11107

(<http://iopscience.iop.org/0305-4470/34/49/325>)

View [the table of contents for this issue](#), or go to the [journal homepage](#) for more

Download details:

IP Address: 171.66.16.101

The article was downloaded on 02/06/2010 at 09:48

Please note that [terms and conditions apply](#).

Stability of lipid bridges

Riccardo Rosso and Epifanio G Virga

Dipartimento di Matematica, Istituto Nazionale di Fisica della Materia, Università di Pavia,
via Ferrata 1, I-27100 Pavia, Italy

Received 31 July 2001, in final form 12 October 2001

Published 30 November 2001

Online at stacks.iop.org/JPhysA/34/11107

Abstract

Lipid bridges are lipid membranes linking two parallel, adhesive walls. For appropriate values of both physical and geometrical parameters, there are two types of such bridges, which look quite different from one another. Here we apply a general condition valid for two-dimensional lipid architectures to show that when the elastic energy density of the lipid membrane is quadratic in the mean curvature, both these bridges are locally stable. Moreover, we give a criterion to decide about their global stability when they happen to coexist at equilibrium.

PACS number: 87.10.+e

1. Introduction

The equilibrium of lipid membranes still offers many problems that are relevant to the mathematical modelling of elementary biological structures.

Amphiphilic molecules are the basic constituents of lipid membranes: they are elongated molecules with a polar, hydrophilic head and a slender, hydrophobic tail. When dispersed in water, the tails of these molecules tend to be packed together, screened from the surrounding water molecules by two families of hydrophilic heads organized in adjacent layers. One of the basic structures that can thus be created is a lipid *bilayer*, consisting of two arrays of molecules with their heads facing the environment (see the sketch in figure 1). Mathematically, lipid bilayers are described as surfaces; they can easily be deformed and take on different conformations, among which are both compact surfaces called *vesicles* and hollow cylinders called *tubules*.

Despite the wealth of studies on the statics of lipid membranes, for which a standard reference is [17], general analytical results concerning the stability of the equilibrium configurations are still missing: essentially, a few special conditions are available, valid either for special membrane shapes [6–9] or within a restricted class of deformations [16]. Only numerical treatments are available for general equilibrium shapes, such as that presented in [4]. Luckily, both vesicles and tubules seldom exhibit a multiplicity of equilibrium configurations under the same external conditions, which would make it mandatory to

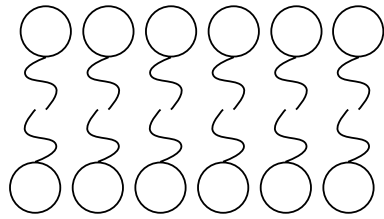


Figure 1. Sketch of a lipid bilayer.

have a criterion to select the shapes that are at least locally stable. Though in [7] the second variation of the elastic energy functional for a lipid membrane has been computed in detail, the problem remains of proving under what conditions this variation is positive definite for all admissible perturbations of an assigned equilibrium configuration of the membrane¹. To our knowledge, such a study of the local stability of lipid membranes is still lacking. We derive in the present paper a general local stability condition valid for a two-dimensional model and we apply it to an equilibrium problem that indeed exhibits more than one solution.

We build upon a method that delivers the exact solution for the equilibrium problem of a lipid membrane in two space dimensions (cf [10–12]). Though this method is especially relevant to straight tubules, similar attempts have also proved useful in the study of vesicles in three-dimensional space (cf [13, 14]). Here we study other possible architectures of lipid membranes, which arise when they bridge two adhesive walls. For tubules, these structures are indeed arches, which can be of two different types, depending on whether the membrane creeps on the walls or not.

We show in section 2 how to establish a criterion for the local stability of the equilibrium configurations of a tubule. In section 3, we illustrate the different equilibrium bridges and determine the critical values of the constitutive parameters that make one prevail energetically over the other. In section 4, we consider a different lipid architecture, where a lipid bridge partially adheres to two misaligned walls; the bridge's ends are further subject to concentrated loads that prevent the bridge from gliding along the walls. Finally, in the appendix we present an alternative analytical method to obtain equilibrium solutions for tubules and, as a curiosity, we show how two classical problems solved by Euler can be given a possibly shorter solution when attacked by this method.

2. Local stability

Lipid membranes are *elastic*, in the sense that their free energy depends on their curvature. Moreover, the molecules in a lipid membrane usually lie in the direction of the unit normal ν to the membrane: sometimes, they can also be oriented by an external agent, such as a magnetic field. Thus, in a general model for lipid membranes the free-energy functional is written in the form

$$F[\mathcal{S}] := \int_{\mathcal{S}} f(H, K, e \cdot \nu) \, da \quad (2.1)$$

¹ To be assured of the technical difficulty of this problem, the reader should heed that the local stability of the sphere for the area functional, which is much simpler than the elastic energy for a membrane, was fully proved less than two decades ago [1].

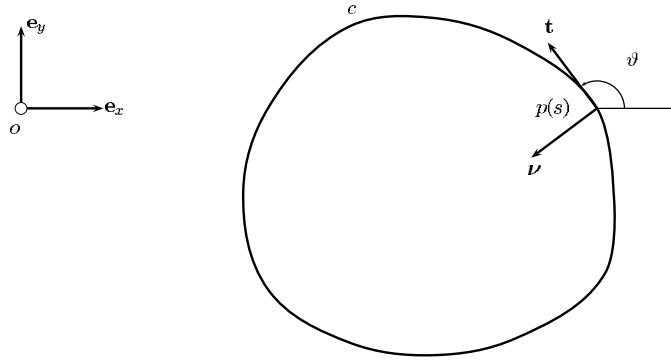


Figure 2. The curve c models a lipid membrane in two space dimensions.

where \mathcal{S} is the surface representing the membrane, a is the area-measure, f is a smooth function of the total curvature $H := \sigma_1 + \sigma_2$ and the Gaussian curvature $K := \sigma_1\sigma_2$ here expressed in terms of the principal curvatures σ_1 and σ_2 of \mathcal{S} and e is a unit vector along a preferred direction, whenever this is present. In the particular case of a tubule, attention can be restricted to any of its transverse sections, which is a plane curve c . The free energy per unit height of the tubule then becomes

$$\mathcal{F}[c] := \int_c \psi(\sigma, \vartheta) ds \quad (2.2)$$

where the function ψ is a specialization of f in (2.1) to the two-dimensional setting we consider here, s is the arc-length on c , σ is the curvature of c and ϑ is the angle between the unit vector t tangent to c and the unit vector e , here taken to lie parallel to the plane of c . Accordingly,

$$\sigma = \vartheta' \quad (2.3)$$

where a prime denotes differentiation with respect to s . The length ℓ of c is regarded as fixed, to mirror the inextensibility of lipid membranes.

Finding a criterion for the local stability of equilibrium membranes requires extending the study in [10]. This is our main objective here. To set the scene we represent the points p of c in the form

$$p(s) - o = x(s)e_x + y(s)e_y \quad (2.4)$$

where o is the origin of the Cartesian frame shown in figure 2 and the preferred direction e is chosen equal to e_x . The unit vectors t and ν , respectively the tangent and normal to c , are described by the formulae

$$t = \cos \vartheta e_x + \sin \vartheta e_y \quad (2.5)$$

and

$$\nu = -\sin \vartheta e_x + \cos \vartheta e_y \quad (2.6)$$

(see figure 2). By (2.3), Frénet–Serret equations immediately follow from (2.5) and (2.6)

$$t' = \sigma \nu \quad \text{and} \quad \nu' = -\sigma t \quad (2.7)$$

where a prime stands for differentiation with respect to s . Since $t = p'$, by differentiating both sides of (2.4), we obtain

$$x' = \cos \vartheta \quad \text{and} \quad y' = \sin \vartheta. \quad (2.8)$$

For a real ε sufficiently small, the curve c is changed into the curve c_ε by the mapping

$$p_\varepsilon = p + \varepsilon \mathbf{u} \quad (2.9)$$

where \mathbf{u} is a smooth vector field on c . To evaluate the functional $\mathcal{F}[c_\varepsilon]$ on c_ε it is necessary to know how the arc-length s_ε and the curvature σ_ε are related to s and σ . Using the formalism employed in [19] we obtain, up to second order in ε ,

$$\frac{ds_\varepsilon}{ds} = 1 + \varepsilon \mathbf{u}' \cdot \mathbf{t} + \frac{1}{2} \varepsilon^2 (\mathbf{u}' \cdot \boldsymbol{\nu})^2 + o(\varepsilon^2) \quad (2.10)$$

which gives the length dilation ratio induced by (2.9). The tangent and normal unit vectors to c_ε are defined as

$$\mathbf{t}_\varepsilon := \frac{dp_\varepsilon}{ds_\varepsilon} \quad \text{and} \quad \boldsymbol{\nu}_\varepsilon := \mathbf{e}_z \wedge \mathbf{t}_\varepsilon$$

where $\mathbf{e}_z := \mathbf{e}_x \wedge \mathbf{e}_y$. Thus, by use of (2.9) and (2.10) we obtain

$$\mathbf{t}_\varepsilon = \mathbf{t} + \varepsilon (\mathbf{u}' \cdot \boldsymbol{\nu}) \boldsymbol{\nu} - \frac{\varepsilon^2}{2} (\mathbf{u}' \cdot \boldsymbol{\nu})^2 \mathbf{t} - \varepsilon^2 (\mathbf{u}' \cdot \mathbf{t}) (\mathbf{u}' \cdot \boldsymbol{\nu}) \boldsymbol{\nu} + o(\varepsilon^2) \quad (2.11)$$

and

$$\boldsymbol{\nu}_\varepsilon = \boldsymbol{\nu} - \varepsilon (\mathbf{u}' \cdot \boldsymbol{\nu}) \mathbf{t} - \frac{\varepsilon^2}{2} (\mathbf{u}' \cdot \boldsymbol{\nu})^2 \boldsymbol{\nu} + \varepsilon^2 (\mathbf{u}' \cdot \mathbf{t}) (\mathbf{u}' \cdot \boldsymbol{\nu}) \mathbf{t} + o(\varepsilon^2). \quad (2.12)$$

Inserting (2.10)–(2.12) into Frénet–Serret equation (2.7)₁, we also arrive at

$$\begin{aligned} \sigma_\varepsilon &= \frac{d\mathbf{t}_\varepsilon}{ds_\varepsilon} \cdot \boldsymbol{\nu}_\varepsilon = \sigma + \varepsilon [(\mathbf{u}' \cdot \boldsymbol{\nu})' - \sigma (\mathbf{u}' \cdot \mathbf{t})] \\ &\quad + \varepsilon^2 \left[\sigma (\mathbf{u}' \cdot \mathbf{t})^2 - \frac{\sigma}{2} (\mathbf{u}' \cdot \boldsymbol{\nu})^2 - (\mathbf{u}' \cdot \mathbf{t}) (\mathbf{u}' \cdot \boldsymbol{\nu})' - [(\mathbf{u}' \cdot \mathbf{t}) (\mathbf{u}' \cdot \boldsymbol{\nu})]' \right] + o(\varepsilon^2). \end{aligned} \quad (2.13)$$

Similarly, it follows from (2.5) and (2.11) that

$$\vartheta_\varepsilon = \vartheta + \varepsilon \mathbf{u}' \cdot \boldsymbol{\nu} - \varepsilon^2 (\mathbf{u}' \cdot \mathbf{t}) (\mathbf{u}' \cdot \boldsymbol{\nu}) + o(\varepsilon^2). \quad (2.14)$$

An equilibrium configuration of c makes \mathcal{F} stationary. Computing as in [11] the first variation of \mathcal{F} with the aid of (2.13) and (2.14), we arrive at the following equilibrium equation:

$$\left[\left(\frac{\partial \psi}{\partial \sigma} \right)' - \frac{\partial \psi}{\partial \vartheta} \right]' - \sigma \left(\lambda + \psi - \sigma \frac{\partial \psi}{\partial \sigma} \right) = 0 \quad (2.15)$$

where λ is an arbitrary constant to be determined by enforcing the constraint on the total length of c . Moreover, it follows from the same computation that the natural boundary conditions at a free end point of c are

$$\frac{\partial \psi}{\partial \sigma} = 0 \quad \frac{\partial \psi}{\partial \vartheta} - \left(\frac{\partial \psi}{\partial \sigma} \right)' = 0 \quad \psi - \sigma \frac{\partial \psi}{\partial \sigma} + \lambda = 0. \quad (2.16)$$

In the appendix we give the mathematical details needed to obtain a special quadrature of (2.15); here we record the result for later use: away from the inflection points where σ vanishes, (2.15) is equivalent to the following transcendental equation for the curvature

$$\psi - \sigma \frac{\partial \psi}{\partial \sigma} + \lambda = \mu \cos \vartheta + \eta \sin \vartheta \quad (2.17)$$

with μ and η arbitrary constants. Together with the multiplier λ , the constants μ and η are to be determined by the geometric constraints imposed on c . In general, they are the total length ℓ and the lengths Δx and Δy spanned by c along the coordinate axes. In the following section,

equation (2.17) will prove useful in finding the equilibrium configurations of a lipid bridge linking two parallel adhesive borders.

To study the local stability of an equilibrium configuration of c we now compute the second variation of \mathcal{F} . For c_ε to be an admissible curve like c , it must have the same total length up to second order in ε , which amounts to requiring that

$$\int_0^\ell \frac{ds_\varepsilon}{ds} ds = \ell + o(\varepsilon^2). \quad (2.18)$$

It is convenient to express \mathbf{u} in the local basis $\{\mathbf{t}, \boldsymbol{\nu}\}$ as

$$\mathbf{u} = u_t \mathbf{t} + u_\nu \boldsymbol{\nu} \quad (2.19)$$

and thence, by virtue of (2.7),

$$\mathbf{u}' = (u_t' - \sigma u_\nu) \mathbf{t} + (\sigma u_t + u_\nu') \boldsymbol{\nu}. \quad (2.20)$$

By (2.10), (2.18) implies that

$$\int_0^\ell \mathbf{u}' \cdot \mathbf{t} ds = 0 \quad \text{and} \quad \int_0^\ell (\mathbf{u}' \cdot \boldsymbol{\nu})^2 ds = 0. \quad (2.21)$$

For closed curves equation (2.21)₁ requires

$$\int_0^\ell \sigma u_\nu ds = 0. \quad (2.22)$$

On the other hand, (2.21)₂ is satisfied if and only if,

$$\mathbf{u}' \cdot \boldsymbol{\nu} = \sigma u_t + u_\nu' \equiv 0 \quad (2.23)$$

which, in particular, implies that

$$\vartheta_\varepsilon = \vartheta + o(\varepsilon^2). \quad (2.24)$$

We thus obtain the second variation of \mathcal{F} :

$$\delta^2 \mathcal{F}(c)[\mathbf{u}] := \left. \frac{d^2}{d\varepsilon^2} \mathcal{F}[c_\varepsilon] \right|_{\varepsilon=0} = \int_0^\ell \sigma^2 \frac{\partial^2 \psi}{\partial \sigma^2} (\mathbf{u}' \cdot \mathbf{t})^2 ds.$$

Since $(\mathbf{u}' \cdot \mathbf{t})$ is completely arbitrary at any given point of an equilibrium curve c , $\delta^2 \mathcal{F}(c)$ is positive definite if and only if,

$$\sigma^2 \frac{\partial^2 \psi}{\partial \sigma^2} > 0 \quad \text{on } c. \quad (2.25)$$

Whenever this inequality is satisfied along an equilibrium configuration c , this is locally stable. Two features of (2.25) are worth noting. First, the dependence of ψ on ϑ does not influence the local stability; this is a consequence of the constraint (2.23) which implies (2.24). Moreover, for a function ψ that depends only on σ , (2.25) is equivalent to requiring that ψ is strictly convex, provided σ never vanishes on c . In particular, in the case where $\psi(\sigma) = \frac{k}{2}(\sigma - \sigma_0)^2$ with a constant σ_0 representing the curvature of an undistorted equilibrium configuration, (2.25) is satisfied or not regardless of the value of σ_0 . Clearly, the local stability criterion expressed by (2.25) becomes ineffective at the inflection points of c .

3. Equilibrium bridges

A lipid *bridge* is a lipid membrane linking two parallel walls, $2R$ apart: we regard it as an open tubule in contact with both walls. The cross-section c of a bridge is a plane curve of length $\ell = 2L$ with one end point on each wall: within our architectural analogy, we call it an *arch*. As shown in figure 2, the arches we consider are all symmetric with respect to the midplane between the walls. The walls are adhesive, so that the arch can be either *simple* or *stilted*: a simple arch touches each wall at a single point (see figure 3(a)), while a stilted arch adheres to each wall along a straight upward segment, called the *stilt* (see figure 3(b)). In the following, we imagine the end points of all simple arches to be fixed on the walls at some selected points which mimic local asperities of the adhering surfaces.

Both simple and stilted arches bear a contact energy at the end points. According to the three-dimensional model described in [13], this energy is due to the splay of the molecules along the membrane's border that reduces the contact between the fluid environment and the hydrophobic tails of the molecules. Assuming that this mechanism is the same for both kinds of arches allows us to neglect its contribution, as it plays no role in determining which is the least energetic. A single stilt bears an adhesion energy \mathcal{F}_a which is given the form

$$\mathcal{F}_a = -wL_* \quad (3.1)$$

where w is the *adhesion potential* of the wall and L_* is the height of the stilt. We assume that both walls have one and the same adhesion potential. By symmetry, we thus study half of the arch c , orienting it from one end point, say p_0 , to the upmost point \hat{p} , as shown in figure 3(a): the length of the half-arch is L and its span across the walls is R . Specifically, the energy functional we consider is

$$\mathcal{F} = \int_0^L \psi(\sigma, \vartheta) ds - wL_* \quad (3.2)$$

subject by (2.8)₁ to the condition

$$\Delta x = \int_0^L \cos \vartheta(s) ds = -R. \quad (3.3)$$

The length L_* is unknown and must be determined so as to minimize \mathcal{F} ; it clearly vanishes for a simple arch.

In particular, here we take

$$\psi = \frac{k}{2}\sigma^2 \quad (3.4)$$

where $k > 0$ is the *bending rigidity* of the membrane, so that, in view of (3.4), (2.17) becomes

$$\sigma = \sqrt{\frac{2}{k}} / \sqrt{\lambda - \mu \cos \vartheta} \quad (3.5)$$

where λ and μ are to be determined by the constraint on the length of the arch and that on the lateral span Δx , whereas η has been set equal to zero because of the symmetry we require of the solution. In fact, $\sigma = -(\frac{2}{k})^{1/2} \sqrt{\lambda - \mu \cos \vartheta}$ is an equilibrium arch too, since it solves (2.17). However, it is symmetric with respect to (3.5) and so it represents the same bridge: indeed, it is changed into (3.5) by turning the walls upside down. Selecting, as we do, the arch with positive curvature is purely conventional. Equation (3.5) must be supplemented by appropriate boundary conditions. By symmetry, for both simple and stilted arches

$$\vartheta|_{\hat{p}} = \pi \quad (3.6)$$

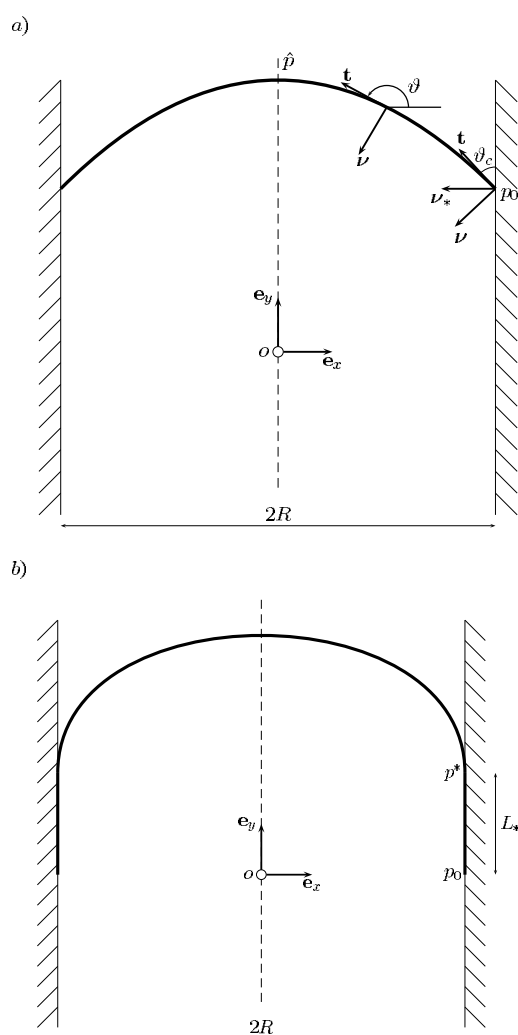


Figure 3. (a) A simple arch; ϑ_c is the contact angle. (b) A stilted arch; L_* is the length of the stilt.

while the boundary conditions at the walls depend on the type of arch being considered. Indeed, they follow from the general equilibrium equations for both the *adhering contour* and the *adhesive border* of an open lipid membrane arrived at in [13]. An adhering contour is every line along which a membrane detaches itself from an adhesive substrate, while an adhesive border is the line where the membrane's border touches the substrate. In general, as explained in detail in [13], adhering contours and adhesive borders may fail to coincide. For the special two-dimensional problem we tackle here, figure 3(b) illustrates the intersections p_0 and p^* of the transverse plane of the bridge with the adhesive border and the adhering contour, respectively. Compared with a simple arch, a stilted arch has the property that the adhering contour and the adhesive border do not coincide. In the following, we separately introduce these boundary conditions and we find the different equilibrium profiles for the lipid bridge that they determine.

3.1. Simple arch

The equilibrium boundary equations for a simple arch follow from those valid along the adhesive border of a lipid membrane on a substrate in three-dimensional space. These conditions have already been derived for a general form of the function f in (2.1) (cf equations (5.13) and (5.14) of [13]). Since the end points of the arch are taken to be fixed, only equation (5.13) of [13] applies here, with ψ as in (3.4). Indeed it amounts to requiring

$$\sigma = 0 \quad \text{at } p_0. \quad (3.7)$$

We define the contact angle ϑ_c of the membrane on the wall so that the outward unit normal ν_* to the wall at p_0 reads

$$\nu_* = \cos \vartheta_c \nu + \sin \vartheta_c t$$

(cf figure 3(a)). The value of ϑ at p_0 , that is, for $s = 0$, is $\vartheta_* := \vartheta_c + \frac{\pi}{2}$; all along the half-arch ϑ ranges in the interval $[\vartheta_*, \pi]$. By (3.5) and (3.7)₂, $\lambda = \mu \cos \vartheta_*$; moreover, μ must be positive for σ to be properly represented by equation (3.5). We thus arrive at

$$\sigma = \sqrt{\frac{2\mu}{k}} \sqrt{\cos \vartheta_* - \cos \vartheta} \quad \text{for } \vartheta \in [\vartheta_*, \pi]. \quad (3.8)$$

The constraints on L and Δx require that

$$L = \sqrt{\frac{k}{2\mu}} \int_{\vartheta_*}^{\pi} \frac{1}{\sqrt{\cos \vartheta_* - \cos \vartheta}} d\vartheta =: g_L(\vartheta_*) \quad (3.9)$$

$$R = -\sqrt{\frac{k}{2\mu}} \int_{\vartheta_*}^{\pi} \frac{\cos \vartheta}{\sqrt{\cos \vartheta_* - \cos \vartheta}} d\vartheta =: g_R(\vartheta_*) \quad (3.10)$$

where use of (2.3) has been made. A first conclusion coming from equations (3.9) and (3.10) is that the ratio $\varrho := \frac{g_L}{g_R}$ is independent of the multiplier μ . It is easily seen that

$$\lim_{\vartheta_* \rightarrow \frac{\pi}{2}^+} \varrho(\vartheta_*) = \varrho_0 \quad \text{and} \quad \lim_{\vartheta_* \rightarrow \pi^-} \varrho(\vartheta_*) = 1$$

where

$$\varrho_0 := \frac{\int_{\frac{\pi}{2}}^{\pi} \frac{1}{\sqrt{-\cos \vartheta}} d\vartheta}{\int_{\frac{\pi}{2}}^{\pi} \sqrt{-\cos \vartheta} d\vartheta} = \frac{\int_0^{\frac{\pi}{2}} \frac{1}{\sqrt{\cos \vartheta}} d\vartheta}{\int_0^{\frac{\pi}{2}} \sqrt{\cos \vartheta} d\vartheta} \simeq 2.19. \quad (3.11)$$

A numerical computation shows that the function ϱ is monotonically decreasing in $]\frac{\pi}{2}, \pi[$, and so it ranges in $[1, \varrho_0]$. Thus, we conclude that no equilibrium simple arch exists whenever the parameter

$$\beta := \frac{L}{R} \quad (3.12)$$

lies outside the interval $[1, \varrho_0]$, whereas, for L/R within this interval, ϑ_* is the unique root of $\varrho(\vartheta_*) = \beta$. For a given ϑ_* , the multiplier μ is then determined by either (3.9) or (3.10). The graph of ϱ in figure 4(a) also shows that, for a prescribed value of R , the contact angle ϑ_c increases from 0 to $\frac{\pi}{2}$ whenever L decreases from $\varrho_0 R$ to R . It is also interesting to note that solutions with different values of L and R , but with the same ratio L/R , can be obtained from one another by simply rescaling the curvature.

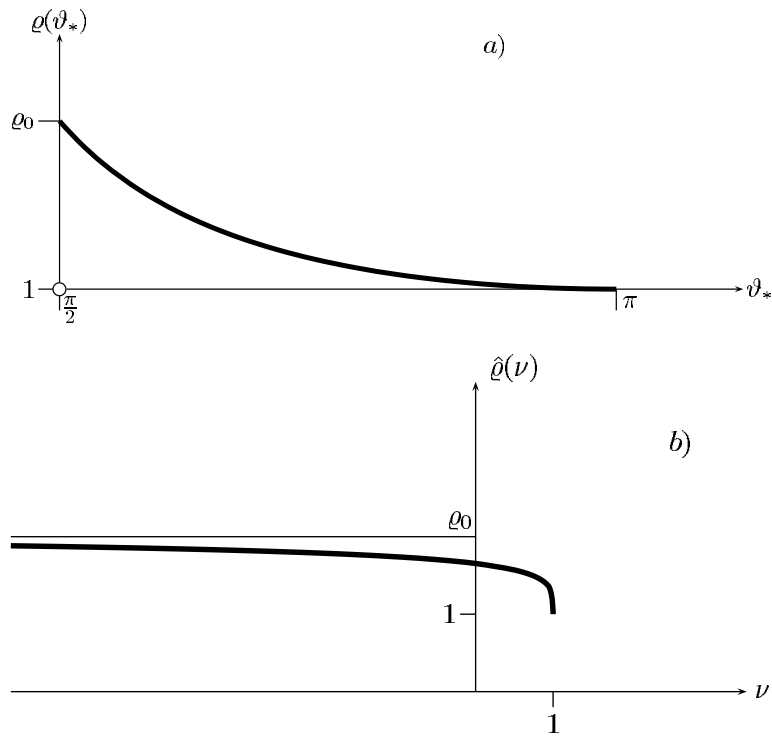


Figure 4. (a) The graph of ϱ against ϑ_* , (b) the graph of $\hat{\varrho}$ against the multiplier ν .

3.2. Stilted arch

As explained above in this section, the equilibrium boundary conditions for a stilted arch also follow from the general equilibrium equations for both the adhering contour and the adhesive border derived in [13].

Since by (3.2) the adhesion energy per unit length is $-w$, it readily follows from equation (5.11) of [13] that

$$\lambda = w \quad \text{at } p_0. \tag{3.13}$$

Similarly, equation (4.14) of [13] yields

$$\sigma^* = \sqrt{\frac{2w}{k}} \quad \text{at } p^* \tag{3.14}$$

where σ^* is the limiting value of σ at p^* taken from the side of the free membrane, and the same convention as in (3.5) has been adopted for the sign of the curvature. In a two-dimensional setting, equation (3.14) was derived in [15] for flat walls and further extended in [12] to arbitrarily curved walls. It is indeed the same as the equilibrium condition found in [18] for axisymmetric vesicles adhering to a flat wall.

By (3.14), equation (3.8) delivers the following expression for the curvature of the equilibrium stilted arch:

$$\sigma = \sqrt{\frac{2w}{k}} \sqrt{1 + \nu \cos \vartheta} \quad \text{for } \vartheta \in \left[\frac{\pi}{2}, \pi \right] \tag{3.15}$$

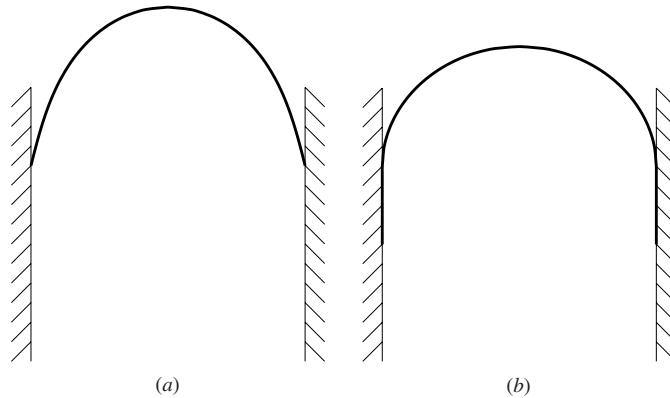


Figure 5. (a) Simple and (b) stilted arches obtained by solving the equilibrium equation.

where $\nu := \frac{\mu}{w}$ must be less than 1 and so chosen that the constraint on Δx be satisfied. By (3.15), (3.3) and (2.3) this constraint becomes

$$\xi(\nu) := - \int_{\frac{\pi}{2}}^{\pi} \frac{\cos \vartheta}{\sqrt{1 + \nu \cos \vartheta}} d\vartheta = \alpha \quad (3.16)$$

where

$$\alpha := \frac{R\sqrt{2w}}{\sqrt{k}}. \quad (3.17)$$

It is easily shown that ξ is a strictly increasing function satisfying

$$\lim_{\nu \rightarrow -\infty} \xi(\nu) = 0 \quad \text{and} \quad \lim_{\nu \rightarrow 1^-} \xi(\nu) = +\infty.$$

This suffices to conclude that for every positive value of α , there is a unique root ν_α of (3.16). Here the constraint on the length of the arch plays the role of a compatibility condition: it must only be ensured that the length of the free arch does not exceed L , that is,

$$L \geq \frac{R}{\alpha} \int_{\frac{\pi}{2}}^{\pi} \frac{1}{\sqrt{1 + \nu \cos \vartheta}} d\vartheta =: \hat{L}(\nu). \quad (3.18)$$

For a given α , the root ν_α of (3.16) is admissible whenever it satisfies (3.18). Paralleling our discussion in the preceding subsection, we plot in figure 4(b) the graph of the function $\hat{\varrho}(\nu) := \frac{\alpha \hat{L}(\nu)}{R \xi(\nu)}$. This is clearly strictly decreasing, and its limits can easily be calculated with the aid of (3.16) and (3.18):

$$\lim_{\nu \rightarrow -\infty} \hat{\varrho}(\nu) = \varrho_0 \quad \text{and} \quad \lim_{\nu \rightarrow 1^-} \hat{\varrho}(\nu) = 1 \quad (3.19)$$

where ϱ_0 is the same as in (3.11).

Figure 5 shows two typical equilibrium arches, corresponding to the same values of both the total length $2L$ and the width $2R$.

3.3. Coexistence

Our aim in this section is to conclude that simple arches can store less elastic free energy than stilted arches. To this end we should first address the question whether simple and stilted equilibrium arches can coexist. The answer to this question is not obvious, because the existence of simple and stilted equilibrium arches is determined by different parameters,

namely β in (3.12) and α in (3.17). Here we show how these parameters should be chosen for simple and stilted arches to coexist.

For every β given in $[1, \varrho_0]$, there is a unique root of the equation $\varrho(\vartheta_*) = \beta$, which we denote by $\hat{\vartheta}_*$. Similarly, figure 4(b) shows that there is a unique value ν_β of ν such that $\hat{\varrho}(\nu_\beta) = \beta$. Thus, for every $\nu \in (\nu_\beta, 1)$, $\hat{\varrho}(\nu)R$ is the length of the free part of an admissible stilted arch, as (3.18) is satisfied. The equilibrium stilted arch then corresponds to the specific value of ν that solves (3.16). Since ξ is a monotonic function, the root of (3.16) ranges in $[\nu_\beta, 1]$, provided that $\alpha \geq \xi(\nu_\beta)$. Moreover, the mapping $\beta \mapsto \nu_\beta$ is monotonically decreasing and so is $\beta \mapsto \xi(\nu_\beta)$. Hence, denoting by $\hat{\beta}$ the inverse of the latter mapping, we can recast the inequality $\alpha \geq \xi(\nu_\beta)$ in the form $\beta \geq \hat{\beta}(\alpha)$.

Simple and stilted equilibrium arches coexist in the region of the (α, β) -plane where $\hat{\beta} \leq \beta \leq \varrho_0$. While for $\beta = \hat{\beta}$ simple and stilted arches are qualitatively different, the stilt's height is zero and so both arches touch each wall at a single point. It is worth noting that for a given separation $2R$ between the walls and for a given length $2L$ of the arch, the condition for the existence of an equilibrium stilted arch amounts to saying that the adhesion potential w of the walls must exceed the critical value

$$w_c := \frac{k\xi^2(\nu_\beta)}{2R^2} \quad \text{for } \beta = \frac{L}{R}.$$

Since for ψ as in (3.4) inequality (2.25) is identically satisfied, both simple and stilted arches are locally stable. We show below that a single line inside the coexistence region marks the global stability transition from one equilibrium arch to the other.

3.4. Stability diagram

For the energy comparison between simple and stilted arches to be meaningful, they need not only coexist but they must also possess the same total length. We shall bear in mind this while computing the free energy of the equilibrium arches in the coexistence region of the (α, β) -plane. In the following, we take α as given and measure all energies in units of $\sqrt{2wk}$.

For $\beta \geq \hat{\beta}(\alpha)$, with the aid of (2.3) and (3.4), we write the dimensionless free energy e of a complete simple arch as

$$e = \sqrt{\frac{k}{2w}} \int_{\hat{\vartheta}_*}^{\pi} \sigma \, d\vartheta \tag{3.20}$$

where σ is as in (3.8). Inserting this latter into (3.20) and making use of both (3.10) and (3.17), we arrive at

$$e = -\frac{1}{\alpha} \int_{\hat{\vartheta}_*}^{\pi} \frac{\cos \vartheta}{\sqrt{\cos \hat{\vartheta}_* - \cos \vartheta}} d\vartheta \int_{\hat{\vartheta}_*}^{\pi} \sqrt{\cos \hat{\vartheta}_* - \cos \vartheta} \, d\vartheta \tag{3.21}$$

where $\hat{\vartheta}_*$ is the unique root of the equation $\varrho(\vartheta_*) = \beta$.

Similarly, by heeding that in (3.2) $L_* = L - L_0$ and resorting to both (3.4) and (3.8), we compute the dimensionless free energy \hat{e} stored in a complete stilted arch as

$$\hat{e} = \int_{\frac{\pi}{2}}^{\pi} \sqrt{1 + \nu \cos \vartheta} \, d\vartheta + \int_{\frac{\pi}{2}}^{\pi} \frac{1}{\sqrt{1 + \nu \cos \vartheta}} \, d\vartheta - \beta \tag{3.22}$$

where ν is the unique root of the equation $\xi(\nu) = \alpha$. The inequality

$$e \leq \hat{e} \tag{3.23}$$

has been studied numerically for $\hat{\beta}(\alpha) \leq \beta \leq \varrho_0$: it turns out to be satisfied only in the shadowed region in figure 6.

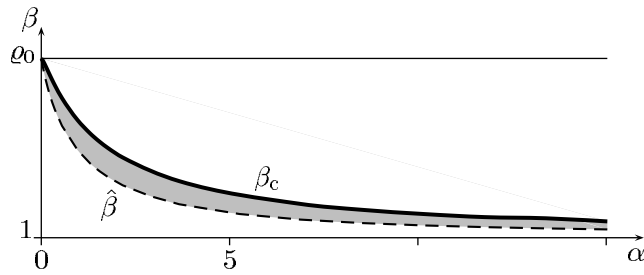


Figure 6. Stability diagram. Simple arches minimize the energy in the shadowed region where $\hat{\beta} \leq \beta \leq \beta_c(\alpha)$, whereas stilted arches minimize the energy when $\beta_c(\alpha) \leq \beta \leq \varrho_0$.

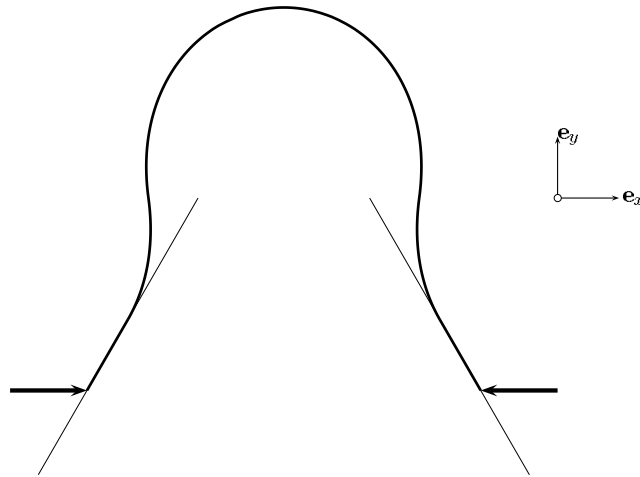


Figure 7. A lipid bridge at equilibrium along a pair of misaligned walls. Here, $w = \gamma$ and $\alpha = \frac{\pi}{6}$.

For every $\alpha \geq 0$, there is a critical value $\beta_c(\alpha)$ of β such that for $\beta_c(\alpha) \leq \beta \leq \varrho_0$ the lipid arch with the least energy is stilted, whereas it is simple for $\hat{\beta} \leq \beta \leq \beta_c(\alpha)$. The critical length $L_c := \beta_c R$ marking this transition between two local energy minimizers decreases when the adhesion potential w increases, showing that a shorter length suffices to make the lipid membrane creep on the walls when these become more adhesive.

4. Misaligned walls

To conclude our study on lipid bridges, we consider here a problem where a bridge adheres to a pair of walls that fail to be parallel and the ends of the bridge are subject to opposite forces of equal magnitude γ , oriented as in figure 7. The energy \mathcal{F}_b associated with the membrane's border can no longer be regarded as constant: it is proportional to the distance between the end points of the curve c :

$$\mathcal{F}_b = \gamma \Delta x = -\gamma \int_0^L \cos \vartheta(s) \, ds.$$

Adding \mathcal{F}_b to the energy functional in (3.2) should prevent the end points of c from gliding on the walls.

Formally, we can still employ the definition of \mathcal{F} in (3.2), provided that ψ is changed to $\tilde{\psi} := \psi - \gamma \cos \vartheta$. Thus, the equilibrium boundary condition for a stilted arch in (3.13) becomes

$$\lambda = w - \gamma \sin \alpha \tag{4.1}$$

since $\vartheta = \frac{\pi}{2} + \alpha$ at the end point p_0 . Moreover, taking ψ as in (3.4), we arrive at the following representation for the equilibrium curve c :

$$\sigma^2 = \frac{2}{k}(w - \gamma(\sin \alpha + \cos \vartheta)). \tag{4.2}$$

It follows from (4.2) that σ vanishes at $\vartheta_0 := \arccos\left(\frac{w}{\gamma} - \sin \alpha\right)$, provided that

$$\frac{w}{\gamma} - \sin \alpha \leq 1. \tag{4.3}$$

This is indeed a necessary condition for an equilibrium curve c to exist, because whenever it is violated ϑ is prevented from attaining π and so (3.6) cannot be satisfied.

As is clear from figure 7, along an equilibrium curve σ starts negative on the wall at $\vartheta = \frac{\pi}{2} + \alpha$, it then changes its sign as ϑ crosses ϑ_0 . As expected, (4.3) gives a critical value of γ below which the lipid membrane would glide on the walls. When (4.3) is satisfied, an equilibrium curve exists whenever L exceeds the critical value L_c given by

$$L_c = 2 \int_{\vartheta_0}^{\frac{\pi}{2} + \alpha} \frac{1}{\sigma} d\vartheta + \int_{\frac{\pi}{2} + \alpha}^{\pi} \frac{1}{\sigma} d\vartheta$$

where σ is the positive root of (4.2).

Appendix

Here we show how equation (2.17) can be obtained by quadrature; we then employ it to solve in an alternative way two classical Euler’s problems.

When the energy per unit length ψ depends only on the curvature σ , equation (2.15) is a special case of the equilibrium equations for a space curve, which reads as

$$\begin{cases} \left(\frac{d\psi}{d\sigma}\right)'' - \sigma\psi - (\tau^2 - \sigma^2)\frac{d\psi}{d\sigma} - \sigma\lambda = 0 \\ \tau\left(\frac{d\psi}{d\sigma}\right)' + \left(\tau\frac{d\psi}{d\sigma}\right)' = 0 \end{cases} \tag{A1}$$

where τ is the torsion of c (see pp 50–53 of [2]). As observed by Radon, it is possible to solve (A1) by quadrature (see pp 53–55 of [2]), retracing the equilibrium curve via successive integrations. The solution, however, is given in a very implicit way, so that it is often difficult to appreciate its qualitative features. For a plane curve, when ψ also depends on ϑ , a better insight into this equilibrium problem can be gained by another special quadrature. It is possible to regard σ as a function of ϑ , at least whenever σ does not vanish. By (2.3), and denoting the differentiation with respect to ϑ by a superimposed dot, we easily arrive at

$$\left[\left(\frac{\partial\psi}{\partial\sigma}\right)' - \frac{\partial\psi}{\partial\vartheta}\right]' = \sigma \left[\left(\frac{\partial\psi}{\partial\sigma}\right)'' + \left(\frac{\partial\psi}{\partial\sigma}\right)' \dot{\sigma} - \left(\frac{\partial\psi}{\partial\vartheta}\right)' \dot{\vartheta}\right] = -\sigma \ddot{f}$$

where

$$f(\vartheta) := \left(\psi - \sigma \frac{d\psi}{d\sigma} + \lambda\right) \tag{A2}$$

and use has been made of the identity

$$\dot{\psi} = \frac{\partial \psi}{\partial \vartheta} + \frac{\partial \psi}{\partial \sigma} \dot{\sigma}.$$

Thus, equation (2.15) takes the form

$$\sigma(\ddot{f} + f) = 0$$

which by (A2) implies equation (2.17), where μ and η are arbitrary constants and $\sigma \neq 0$.

This is the analytical counterpart of the method employed in [10, 11] that rephrases the variational problem for \mathcal{F} in terms of the focal curve associated with c . The only difference is that in the equilibrium equation arrived at in [10] the constants λ , μ and η are all zero, as in the variations of c performed there the end points of an isolated perturbed arc *glide* along c , and so all geometric constraints are locally relaxed. A glance at (2.8) suffices to show that the right-hand side of (2.17) actually reconciles the geometric and analytic approaches to this equilibrium problem, as fixing the end points of a perturbed arc a on c —possibly the whole of c —just amounts to prescribing the values of the integrals

$$\int_a \cos \vartheta \, ds \quad \text{and} \quad \int_a \sin \vartheta \, ds.$$

Equation (2.17) is equivalent to (2.15) but, at variance with this, it makes it easy to determine all null Lagrangians for \mathcal{F} . In fact,

$$\varphi_0(\sigma, \vartheta) := g(\vartheta)\sigma - \lambda + \mu \cos \vartheta + \nu \sin \vartheta$$

with g any smooth function and λ , μ and ν arbitrary constants, is clearly the most general energy density that renders (2.17) identically satisfied, and so adding it to any function ψ would not affect the equilibrium equation for c , as could also be checked by a direct computation in (2.15). Below, we apply equation (2.17) to two classical equilibrium problems.

Elastica

The first problem is Euler's *elastica*. Consider an inextensible, flexible rod welded upright to a horizontal wall at one end and subject to the downward vertical load $\mathbf{P} = -P\mathbf{e}_y$ at the opposite end (see figure 8).

The energy functional for the curve c that represents the rod is

$$\mathcal{F}[c] = \int_0^L \frac{1}{2}k\sigma^2 \, ds + Py(L) \quad (\text{A3})$$

which, by (2.8)₂, can be given the form (2.2) with

$$\psi = \frac{1}{2}k\sigma^2 + P \sin \vartheta. \quad (\text{A4})$$

Since the only geometric constraint on c is its length L , we set both μ and η equal to zero in equation (2.17); for ψ as in (A4), this equation yields

$$\sigma = \sqrt{\frac{2}{k}(\lambda + P \sin \vartheta)} \quad (\text{A5})$$

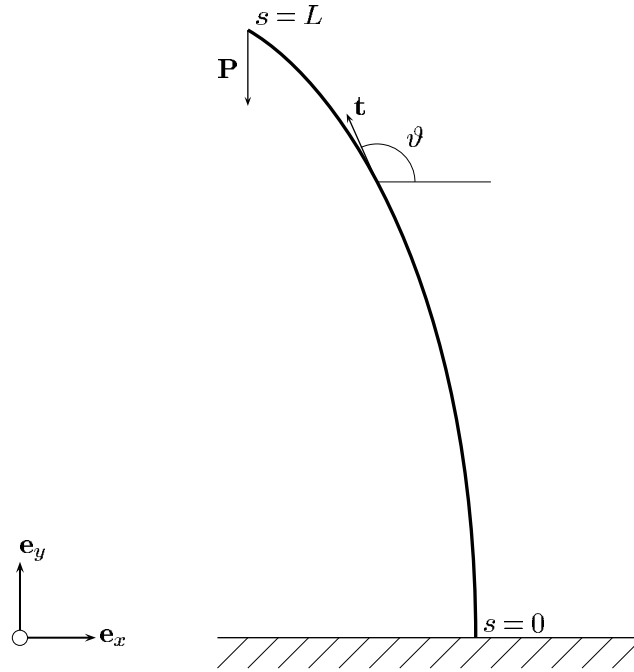


Figure 8. A flexible rod loaded at one end point.

with $\frac{\pi}{2} \leq \vartheta \leq \vartheta_0$, for the solution with positive curvature depicted in figure 8 (the other solution, which has opposite curvature, represents a curve symmetric to this). Equation (A5) represents the first integral of equation (2.15), which in the present setting reads

$$k\sigma'' + \frac{1}{2}k\sigma^3 - \lambda\sigma = 0. \quad (\text{A6})$$

As expected, this equation does not depend on P because $\sin \vartheta$ is a null Lagrangian for \mathcal{F} . It is worth noting that (A6) and the classical equilibrium equation for the elastica (cf e.g. (8) on p 401 of [5]) have the same solutions, as they both enjoy the same first integral (cf (9) of [5]). Here the natural boundary conditions (2.16) are to be enforced at $s = L$. Combining (A4), (A5) and (2.16)₁, we conclude that $\lambda = -P \sin \vartheta_0$, while both (2.16)_{1,2} are identically satisfied along c . We then readily determine ϑ_0 , by requiring that

$$L = \int_{\frac{\pi}{2}}^{\vartheta_0} \frac{1}{\sigma} d\vartheta = \sqrt{\frac{k}{2P}} \int_{\frac{\pi}{2}}^{\vartheta_0} \frac{1}{\sqrt{\sin \vartheta - \sin \vartheta_0}} d\vartheta = \sqrt{\frac{k}{P}} K \left(\frac{1}{2} \sqrt{1 - \sin \vartheta_0} \right) \quad (\text{A8})$$

where K is the complete elliptic integral of the first kind. Since K is a strictly increasing function, there is precisely one root ϑ_0 of (A8), provided that

$$L \geq \sqrt{\frac{k}{P}} K(0) = \sqrt{\frac{k}{P}} \frac{\pi}{2}$$

which delivers the classical critical load $P_c = \frac{k\pi^2}{4L^2}$ for the rod to start bending.

Cycloid

Euler also posed the problem of finding a plane curve c such that the area swept out by its radii of curvature has minimum value (see e.g. [3], p 66). The energy functional for this problem is

$$\mathcal{F}[c] = \int_0^L \frac{1}{\sigma} ds.$$

In the absence of the constraint on the length of c , equation (2.17) yields

$$\sigma = \frac{1}{\mu \cos \vartheta + \eta \sin \vartheta}$$

which setting $\eta = \mu \tan \alpha$ transforms into the equation for a cycloid:

$$\sigma = \frac{\cos \alpha}{\mu \cos(\vartheta - \alpha)}.$$

References

- [1] Barbosa J L and do Carmo M P 1984 Stability of hypersurfaces of with constant mean curvature *Math. Z.* **185** 339
- [2] Blaschke W 1930 *Vorlesungen über Differentialgeometrie* vol 1 (Berlin: Springer)
- [3] Giaquinta M and Hildebrandt S 1996 *Calculus of Variations I* (Berlin: Springer)
- [4] Jarić M, Seifert U, Wintz W and Wortis M 1995 Vesicular instabilities: the prolate-to-oblate transition and other shape instabilities of fluid bilayer membranes *Phys. Rev. E* **52** 6623
- [5] Love A E H 1944 *A Treatise on the Mathematical Theory of Elasticity* (New York: Dover)
- [6] Ou-Yang Z-c and Helfrich W 1987 Instability and deformation of a spherical vesicle by pressure *Phys. Rev. Lett.* **59** 2486
- [7] Ou-Yang Z-c and Helfrich W 1989 Bending energy of vesicle membranes: general expressions for the first, second, and third variation of the shape energy and applications to spheres and cylinders *Phys. Rev. A* **39** 5280
- [8] Peterson M 1985 Geometrical methods for the elasticity theory of membranes *J. Math. Phys.* **26** 711
- [9] Peterson M 1985 An instability of the red blood cell shape *J. Appl. Phys.* **57** 1739
- [10] Rosso R and Virga E G 1998 Adhesion of tubules in an assembly *Eur. J. Appl. Math.* **9** 485
Rosso R and Virga E G 1998 *Eur. J. Appl. Math.* **10** 221 (erratum)
- [11] Rosso R and Virga E G 1998 Exact statics and approximate dynamics of adhering lipid tubules *Contin. Mech. Thermodyn.* **10** 107
- [12] Rosso R and Virga E G 1998 Adhesion by curvature of lipid tubules *Contin. Mech. Thermodyn.* **10** 359
- [13] Rosso R and Virga E G 1999 Adhesive borders of lipid membranes *Proc. R. Soc. A* **455** 4145
- [14] Rosso R and Virga E G 2000 Squeezing and stretching of lipid membranes *J. Phys. A: Math. Gen.* **33** 1459
- [15] Seifert U 1991 Adhesion of vesicles in two dimensions *Phys. Rev. A* **43** 6803
- [16] Seifert U 1991 Conformal transformations of vesicle shapes *J. Phys. A: Math. Gen.* **24** L573
- [17] Seifert U 1997 Configurations of fluid membranes and vesicles *Adv. Phys.* **46** 13
- [18] Seifert U and Lipowsky R 1990 Adhesion of vesicles *Phys. Rev. A* **42** 4768
- [19] Virga E G and Fournier J-B 1995 Equilibrium confocal textures in a smectic-A cell *Rend. Mat. Acc. Lincei* **6** series IX 65